

# LiCu<sub>x</sub>Mn<sub>2-x</sub>O<sub>4</sub> Spinel (0.1 ≤ x ≤ 0.5): A New Class of Cathode Materials for Li Batteries

## II. In Situ Measurements

Yair Ein-Eli,\*<sup>a</sup> Sharon H. Lu, and Maria A. Rzeznik

Covalent Associates, Incorporated, Woburn, Massachusetts 01801, USA

Sanjeev Mukerjee,\* Xiao Q. Yang,\* and James McBreen\*

Brookhaven National Laboratory, Upton, New York 11973-5000, USA

### ABSTRACT

Electrochemical data obtained from lithium cycling in LiCu<sub>x</sub>Mn<sub>2-x</sub>O<sub>4</sub> spinels (0.1 ≤ x ≤ 0.5) show a remarkable, highly reversible, electrochemical cycling behavior at 4.9 V. In situ X-ray absorption near edge structure spectroscopy revealed that this ultrahigh voltage is due to the existence of the Cu<sup>2+</sup>/Cu<sup>3+</sup> redox couple. The origin of the high stability at the 5 V region was studied with the in situ X-ray diffraction technique. It was found that the unit cell dimension undergoes minimal change during charge-discharge cycles at the 5 V plateau.

### Introduction

In our earlier communications<sup>1,2</sup> we reported on novel electroactive materials, LiCu<sub>x</sub>Mn<sub>2-x</sub>O<sub>4</sub> (0.1 ≤ x ≤ 0.5). The electrochemical data obtained from lithium cells containing these materials as cathodes (positive electrodes) showed that lithium ions can be extracted from the spinel structure in two main potential regions: the first, at the sloping region of 3.9 to 4.3 V, was attributed to the oxidation of Mn<sup>3+</sup> to Mn<sup>4+</sup>, whereas the second potential plateau, observed at 4.8 to 5 V, was assigned to the oxidation of Cu<sup>2+</sup> to Cu<sup>3+</sup>. These electrochemical reactions are highly reversible, and stable electrochemical cycling observed. We found that the stability of the electrodes during cycling depended on the composition of the material, i.e., stable electrochemical cycling was observed for electrodes with high values of x in LiCu<sub>x</sub>Mn<sub>2-x</sub>O<sub>4</sub>. However, the composition with x = 0.5 (LiCu<sub>0.5</sub>Mn<sub>1.5</sub>O<sub>4</sub>) exhibits an overall capacity of about 70 mAh/g and of this only 25 mAh/g were obtained at the 4.9 V plateau. X-ray and neutron diffraction data along with x-ray absorption near edge structure (XANES) spectroscopy showed that it is very difficult to synthesize single-phase lithium-copper-manganese oxide spinel compounds with a predetermined composition. These studies revealed that the cation distribution in these spinel compounds is extremely complex because the stability and relatively low reactivity of CuO, compared to Li<sub>2</sub>O, appears to restrict complete incorporation of copper into the spinel structure.<sup>2</sup>

In this paper we provide evidence that the remarkable reversible electrochemical reaction occurring at the potential of 5 V is attributable solely to the oxidation of Cu<sup>2+</sup> to Cu<sup>3+</sup>. In situ XANES spectra of these spinels were obtained at the low (3.9–4.3 V) and the ultrahigh (4.8–5 V) potential plateaus. We also conducted in situ X-ray diffraction (XRD) measurements and evaluated the unique morphology developed in order to detect the origin of the high stability of these novel electrodes upon cycling in Li cells.

### Experimental

LiCu<sub>x</sub>Mn<sub>2-x</sub>O<sub>4</sub> (0.1 ≤ x ≤ 0.5) cathode materials were prepared by solid-state and sol-gel methods and were studied electrochemically as described previously in Ref. 2. The electrolyte composition was 1 M LiPF<sub>6</sub> in a mixture of ethylene carbonate (EC) and ethyl methyl carbonate (EMC) (EM Industries) in a volume ratio of 1 EC:3 EMC.

*In situ XRD and XANES Measurements.*—LiCu<sub>0.5</sub>Mn<sub>1.5</sub>O<sub>4</sub> electrodes (2.85 cm<sup>2</sup>) were assembled into cells with the use of lithium metal as anodes (negative electrodes). The cells

\* Electrochemical Society Active Member.

<sup>a</sup> Present address: Electric Fuel Limited, Beit-Shemesh, 99000 Israel.

were charged and discharged at a low current density of ~50 μA/cm<sup>2</sup>. In situ XRD measurements were conducted at Beam Line X18A as reported in Ref. 3, and the in situ XAS was performed at Beam Line X11A of NSLS as was described in Ref. 4. The XRD measurements were carried out in the transmission mode with a 10.375 keV (λ = 1.195 Å) X-ray beam. Successive scans were recorded between 2θ values of 43 to 53° as the cells were cycled. The scan included the (333) and (511) peaks of the spinel, which coincide, as well as the (440) and (531) peaks. Also included was the aluminum (220) peak, which was used as an internal standard. In situ XAS measurements were carried out in the transmission mode at various stages of charge at both the Mn and Cu K edges. Three detectors were used with a calibration sample (Mn or Cu) for alignment of edge spectra as described in Ref. 2.

Scanning electron microscopy (SEM, Amray 1810) was used to examine the morphology of the LiCu<sub>x</sub>Mn<sub>2-x</sub>O<sub>4</sub> powder and its effect on electrochemical performance.

### Results and Discussion

Figure 1a and b displays the good electrochemical behavior of the copper-modified spinel LiCu<sub>0.5</sub>Mn<sub>1.5</sub>O<sub>4</sub>. This material exhibits long cycle life (more than 200 cycles) with a rather low capacity fade rate. Our data indicate that capacity loss at the 5 V potential plateau is mainly responsible for the observed capacity fade. The capacity fade, observed upon cycling, could be attributed to electrolyte oxidation occurring at this ultrahigh potential. However, as can be seen in Fig. 1b, the cell could be cycled initially at the 5 V potential region without any significant change in the cell potential upon polarization.

In order to understand the reasons for the high cycling stability of the copper-modified spinel in Li cells, we first examined the morphology of these materials.

*Morphological characterization of the Cu-modified spinel.*—A series of scanning electron microscopy (SEM) micrographs obtained from the unmodified LiMn<sub>2</sub>O<sub>4</sub> spinel and the LiCu<sub>x</sub>Mn<sub>2-x</sub>O<sub>4</sub> compositions (0.2 ≤ x ≤ 0.5), prepared via solid-state technique, is presented in Fig. 2. The unmodified spinel (Fig. 2a) possesses an onion-like microstructure with approximately 2 μm ring thickness. The copper-modified spinels (Fig. 2b–d) show larger rings with a width of 10–15 μm as well as the formation of a radial microstructure, detectable at x = 0.4 in LiCu<sub>x</sub>Mn<sub>2-x</sub>O<sub>4</sub>. The morphological changes observed in the copper-modified spinels are a function of the amount of copper (x) introduced into the LiCu<sub>x</sub>Mn<sub>2-x</sub>O<sub>4</sub> lattice. As was shown previously,<sup>1,2</sup> increasingly stable cycle life was observed as the copper fraction was increased. The tightly

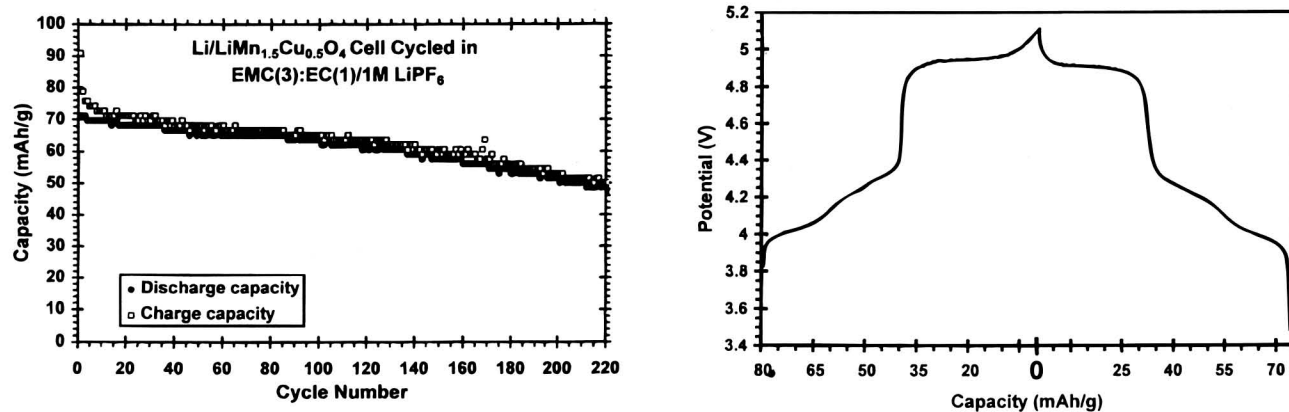


Fig. 1. (a, left) The cycle life characteristic [capacity (mAh/g) vs. cycle number] of "LiMn<sub>1.5</sub>Cu<sub>0.5</sub>O<sub>4</sub>" cathode material cycled vs. Li metal in EMC(3):EC(1)/1 M LiPF<sub>6</sub>. The cell was cycled at a current density of 250  $\mu$ A/cm<sup>2</sup> (C/2) in the potential range of 3.3–5.1 V. (b, right) The potential (V)-capacity (mAh/g) profiles obtained from the third charge-discharge cycle of the same cell.

layered onion-like morphology of LiMn<sub>2</sub>O<sub>4</sub> is subject to cracking unless the lattice, "breathing" from Li-ion intercalation-deintercalation, is extremely well coordinated. With the inclusion of copper in the spinel, and as the Cu content rises towards 25 mol %, the nested shells become wider and more diffuse, with the appearance of radial

microstructure. This type of morphology should be more compatible with expansion/contraction cycles.

*In situ XRD measurements.*—Figure 3 shows the XRD patterns obtained from LiCu<sub>0.5</sub>Mn<sub>1.5</sub>O<sub>4</sub> during the second charge cycle. The charging process was terminated after

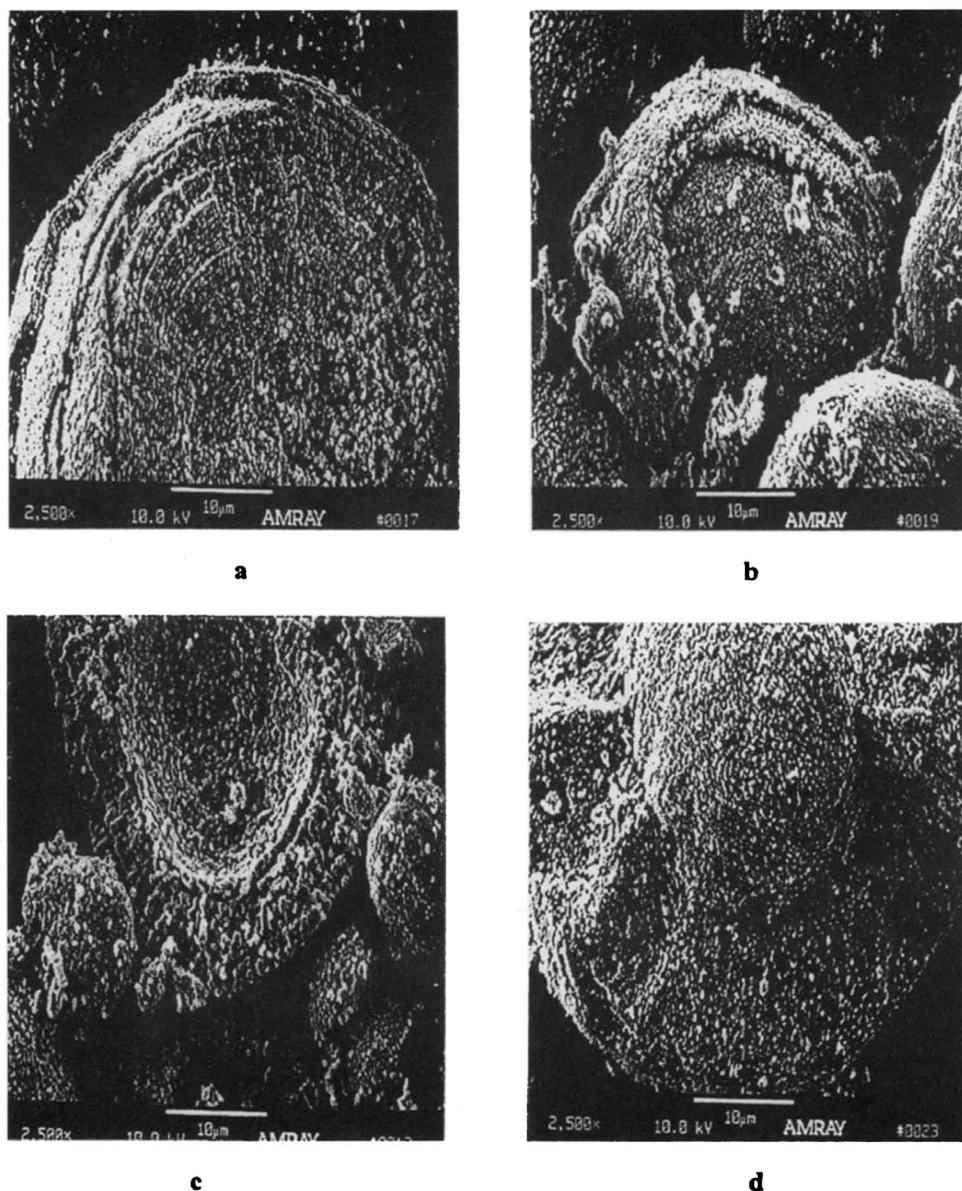


Fig. 2. SEM micrographs obtained from the unmodified LiMn<sub>2</sub>O<sub>4</sub> spinel (a) and the LiMn<sub>2-x</sub>Cu<sub>x</sub>O<sub>4</sub> series (0.2 ≤ x ≤ 0.5; b-d), prepared via solid-state techniques.

### LiCu<sub>0.5</sub>Mn<sub>1.5</sub>O<sub>4</sub> - *In situ* XRD Measurements Charge Step

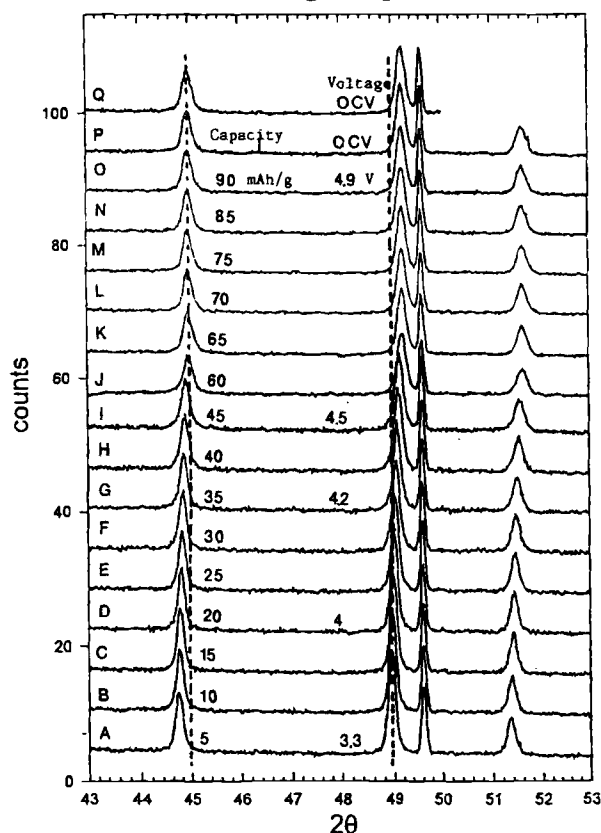


Fig. 3. *In situ* XRD patterns obtained from LiMn<sub>1.5</sub>Cu<sub>0.5</sub>O<sub>4</sub> during the second charge cycle. The last two scans (P and Q) were recorded at open-circuit voltage of 4.9 V after charging was completed.

10.25 h, corresponding to a C/10 rate. The last two scans (P and Q) were taken at open-circuit voltage (ocv) of 4.9 V after charging was completed. The diffraction patterns obtained at the lower sloping potential region (diffraction patterns A-I, corresponding to 3.9–4.5 V) show that the diffraction peaks were shifted to higher angles, indicating a contraction of the lattice upon removal of lithium ions. On the contrary, at the upper potential plateau (XRD patterns J-O, corresponding to 4.8–5 V) no shifts in the diffraction peaks were observed, indicating that the lattice parameters remain constant upon removal of lithium ions at the 5 V potential plateau. Moreover, no evidence was found for the formation of a second cubic phase that is often seen on charging of LiMn<sub>2</sub>O<sub>4</sub> spinel cathode materials to 5 V.<sup>5,6</sup> The peaks observed in the diffraction patterns obtained from the as-prepared powder (XRD pattern A) and from the lower sloping potential region (XRD patterns B-H) are sharper than the diffraction peaks obtained from the high-potential plateau (XRD patterns I-Q). The XRD peak broadening at the high-potential plateau may indicate that some structural changes are taking place during the first charging process. One can attribute these crystallographic changes to cation exchange between A site and B site. The last two XRD patterns (P and Q) were recorded at an OCV of 4.9 V before the cell was polarized, and no shift in the peak position was observed.

Figure 4 presents the corresponding XRD patterns obtained once the Li/LiCu<sub>0.5</sub>Mn<sub>1.5</sub>O<sub>4</sub> cell was discharged at a C/8 rate. Because of a beam dump, no data were collected between 4.4 and 6.05 h, the time between XRD patterns H and I. As can be seen, the process is reversible. The lattice, it appears, does not breathe at the higher potential plateau (XRD patterns A-E). Expansion of the unit cell takes place only below the potential of 4.5 V (XRD patterns F-L). We can conclude that the stability of the LiCu<sub>0.5</sub>Mn<sub>1.5</sub>O<sub>4</sub> upon

### LiCu<sub>0.5</sub>Mn<sub>1.5</sub>O<sub>4</sub> - *In situ* XRD Measurements Discharge Step

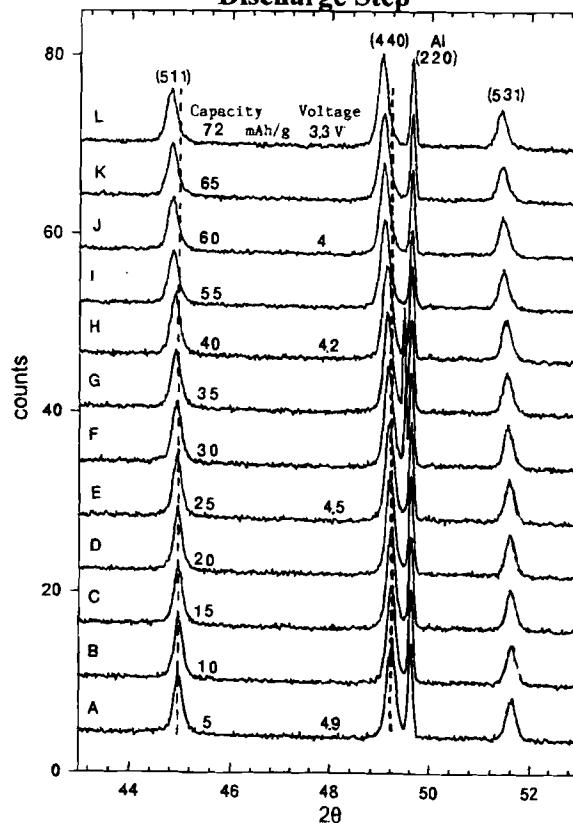


Fig. 4. *In situ* XRD patterns obtained from LiMn<sub>1.5</sub>Cu<sub>0.5</sub>O<sub>4</sub> during the second discharge cycle.

cycling can be attributed to the fact that its lattice does not appear to expand and contract during charging and discharging at the 5 V potential plateau. This behavior resembles that observed with the enriched Li spinels of the type Li<sub>1-x</sub>M<sub>3</sub>O<sub>12</sub> [M=Ti, Mn] (or alternatively, Li[M<sub>1-67</sub>Li<sub>0.33</sub>]O<sub>4</sub>).<sup>7</sup> These materials were observed to be extremely stable upon cycling. This behavior was attributed to the fact that the cubic unit cell does not appreciably expand or contract upon consecutive charge and discharge processes.<sup>8,9</sup> Moreover, the structural analysis of the LiCu<sub>0.5</sub>Mn<sub>1.5</sub>O<sub>4</sub> material revealed that the actual stoichiometry was Li<sub>1.01</sub>Cu<sub>0.32</sub>Mn<sub>1.67</sub>O<sub>4</sub>.<sup>2</sup> Therefore, it is significant that this structure corresponds to the enriched Li spinel compositions mentioned above.

*In situ XANES measurements.*—Figure 5 shows XANES data obtained from LiCu<sub>0.5</sub>Mn<sub>1.5</sub>O<sub>4</sub> at the Mn K edge. At the lower potential plateau (3.9–4.5 V) we observe a shift of 1 eV in the Mn K edge to higher energies, consistent with the conversion of Mn(III) to Mn(IV).<sup>2</sup> Once the potential reaches the upper voltage plateau (4.8–5 V) there is no further shift evident in the edge position. However, the intensity of the white line increases. This behavior indicates a change in the symmetry of the Mn-O coordination occurring at the 4.9–5 V plateau.

Figure 6 presents the XANES data obtained for LiCu<sub>0.5</sub>Mn<sub>1.5</sub>O<sub>4</sub> at the Cu K edge. At the lower potential plateau (3.9–4.3 V) we observe changes in the edge features but no significant changes in the Cu-O coordination expected from the oxidation of Mn(III) to Mn(IV) are visible. At the upper potential plateau (4.8–5 V) we observe a considerable shift of 2 eV in the position of the white line. This shift in the position of the white line is consistent with the oxidation of Cu(II) to Cu(III).<sup>10</sup>

Figure 7 shows the XANES data obtained from LiCu<sub>0.5</sub>Mn<sub>1.5</sub>O<sub>4</sub> at the Cu K edge. The figure presents the data obtained at 3.3 V, before the charge step, and at the

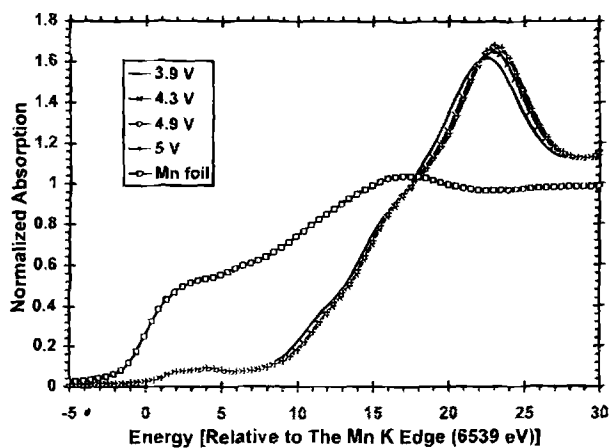


Fig. 5. In situ XANES data obtained from  $\text{LiCu}_{0.5}\text{Mn}_{1.5}\text{O}_4$  at the Mn K edge.

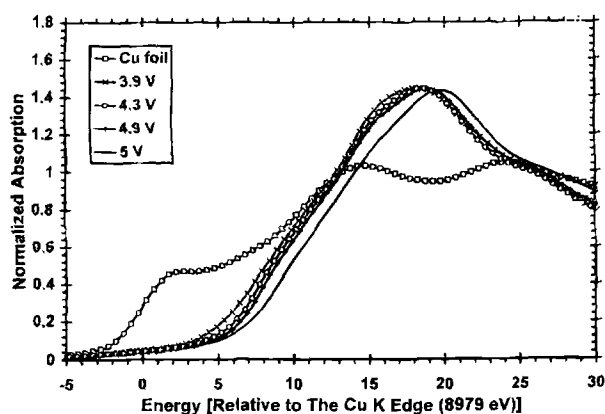


Fig. 6. In situ XANES data obtained for  $\text{LiCu}_{0.5}\text{Mn}_{1.5}\text{O}_4$  at the Cu K edge.

end of the charge process (5 V). Also included in this figure are the spectra obtained from Cu foil [Cu],  $\text{Cu}_2\text{O}$  [Cu(I)], and  $\text{CuO}$  [Cu(II)]. Based on the XANES spectra obtained for these materials we conclude that the 5 V plateau is due solely to the oxidation and reduction of Cu(II)/Cu(III) couple.

### Conclusions

The XRD and XANES results indicate that when  $\text{LiCu}_{0.5}\text{Mn}_{1.5}\text{O}_4$  is cycled at the lower potential region (3.9–4.5 V), Mn(III) is oxidized to Mn(IV). At this potential range the lattice contracts as Li ions are removed from the lattice. At the upper potential plateau (4.8–5 V) no further changes in the Mn oxidation state occur, while Cu(II) is oxidized to Cu(III) without any further contraction of the lattice.

The oxidation of Mn observed at the lower potential plateau (3.9–4.5 V) modifies the coordination symmetry around the copper. The oxidation of Cu, taking place at the ultrahigh potentials (4.8–5 V), modifies the coordination symmetry around the Mn. All of these processes are reversible and occur while maintaining a single cubic spinel phase.

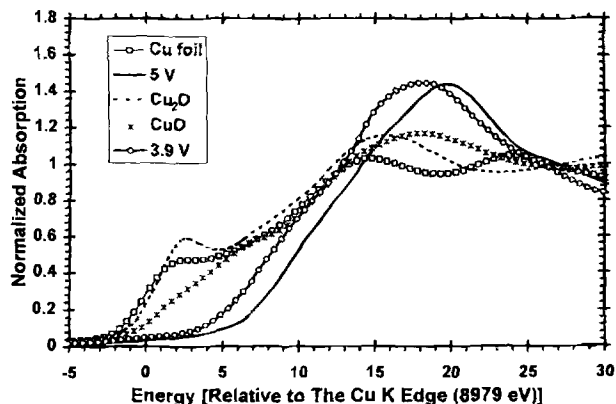


Fig. 7. XANES data obtained at the K edge from  $\text{LiCu}_{0.5}\text{Mn}_{1.5}\text{O}_4$  at 3.3 V, before any charge step, and at the end of the charge process (5 V). Also presented are data obtained from Cu foil [Cu],  $\text{Cu}_2\text{O}$  [Cu(I)], and  $\text{CuO}$  [Cu(II)].

### Acknowledgments

This work was performed under an SBIR Phase I DoD program sponsored by the U.S. Army CECOM, administered by the Army Research Laboratory, Fort Monmouth, New Jersey, under contract no. DAABO7-97-C-D304. The XAS measurements were done at Beam Line X11A, and XRD measurements were conducted at Beam Line X18A, both at NSLS. The work at BNL was supported by the Assistant Secretary for Energy Efficiency and Renewable Energy, Office of Transportation Technologies, Electric and Hybrid Propulsion Division, USDOE under contract no. DE-AC02-76CH00016. We thank Dr. M. M. Thackeray for useful and stimulating discussions.

Manuscript submitted March 27, 1998; revised manuscript received May 26, 1998.

Covalent Associates, Incorporated, assisted in meeting the publication costs of this article.

### REFERENCES

1. Y. Ein-Eli and W. F. Howard, *J. Electrochem. Soc.*, **144**, L205 (1997).
2. Y. Ein-Eli, W. F. Howard, S. H. Lu, S. Mukerjee, J. McBreen, J. T. Vaughey, and M. M. Thackeray, *J. Electrochem. Soc.*, **145**, 1238 (1998).
3. S. Mukerjee, T. R. Thurston, N. M. Jisrawi, X. Q. Yang, J. McBreen, M. L. Daroux, and X. K. Xing, *J. Electrochem. Soc.*, **145**, 466 (1998).
4. Y. Mo, Y. Hu, I. T. Bae, B. Miller, M. R. Antonio, and D. A. Scherson, *J. Electrochem. Soc.*, **144**, 1598 (1997).
5. Y. Xia and M. Yoshio, *J. Electrochem. Soc.*, **143**, 825 (1996).
6. M. N. Richard, I. Koetschau, and J. R. Dahn, *J. Electrochem. Soc.*, **144**, 4554 (1997).
7. T. Ohzuku, A. Ueda, and N. Yamamoto, *J. Electrochem. Soc.*, **142**, 1431 (1995).
8. M. M. Thackeray, A. de Koch, M. H. Rossouw, D. C. Liles, D. Hoge, and R. Bittihn, *J. Electrochem. Soc.*, **139**, 363 (1992).
9. K. M. Kolbow, J. R. Dahn, and R. R. Haering, *J. Power Sources*, **26**, 397 (1989).
10. J. M. Tranquada, S. M. Heald, and A. R. Moodenbaugh, *Phys. Rev. B*, **36**, 5263 (1987).